International Journal of Control and Automation
Vol.8, No.8 (2015), pp.409-424
http://dx.doi.org/10.14257/ijca.2015.8.8.38

PI Predictive Functional Attitude Control of Near Space Vehicle

Zhenyu Lu[1], Kai Li[1], Tingya Yang[2], Wei Guo[3], Jin Wang[1]

[1] *School of Electrical and Information Engineering, Nanjing University of Information Science & Technology, Nanjing 210044, China*
[2] *Jiangsu Meteorological Observatory, Nanjing 210008, China*
[3] *School of Information and Control, Nanjing University of Information Science & Technology, Nanjing 210044, China*

Abstract

Predictive functional control and multivariate PI predictive functional control is presented based on state space equation for non-linear, fast time-varying, multivariable coupling near-space vehicle attitude control system. Transforming nonlinear optimal problems into online optimization in the linear time-invariant systems and solve the control law in a rolling way. Lyapunov's second stability theorem proved that the solved control law can ensure a certain degree of robustness of the closed-loop system. Tuning parameters of multivariable PI predictive functional controller based on particle swarm optimization algorithm. Designed near-space vehicle attitude controller and simulate it. Results show that both of the two control strategy can get good control performance, comparatively, multivariable PI predictive functional control has a better control effect. It has the advantages of non-overshoots, faster response, and smaller steady state error etc.

Keywords: *Near-space vehicle, predictive functional control, attitude control, PI, particle swarm optimization*

1. Introduction

Near-space vehicle (NSV) is the aircraft that can sustain flight and complete a certain mission. When on the mission, NSV's shape, aerodynamic characteristics and flight environment etc are constantly changing that it shows strong nonlinearity, fast time-varying and uncertainty[1-2]. It increased the difficulty of designing attitude control. Traditional control techniques (such as PID) with higher requirements on the object model and can not solve the effects of nonlinear and time-varying factors also its control efficiency can not meet the control requirements of current aircraft.

Model predictive control has been widely control in chemical, petroleum, aviation and other fields [3-4] for its advantages of not strongly depending on model and forward-looking, etc. [5] Discussed the single-step predictive control method for the attitude maneuver of a flexible spacecraft. [6] Designed continuous nonlinear predictive control method based on SDRE and applied to vehicle re-entry attitude control system, however, it needs Lie derivative that increased the amount of calculation.

The traditional predictive control method is computationally intensive and may be accompanied by an unknown control law. As the third-generation model predictive control algorithm, Predictive functional control (PFC) still has the characteristics of model predictive control algorithm. And the difference is that it structuralized control inputs. PFC avoids the unknown control input problem of the other model predictive control, reduces on line computation and improves the system response speed. Most of the existing literature applied PFC on simple input simple output (SISO) system [7-8], while there are few researches studying on multiple-input multiple-output (MIMO) system.

ISSN: 2005-4297 IJCA

Derived multivariate predictive functional control base on transfer function, this paper derived multivariable predictive functional control based on state space equation and applied to the near space vehicle attitude control. Simulation results show that the graphical have overshoot, static state error and frequent shocks which are detrimental to aircraft control. In order to overcome these shortcomings, improved control algorithm—multivariable PI predictive functional control algorithm is proposed. Lyapunov second theorem proved the closed-loop robust stability by the proposed control method. The new algorithm increased the adjustable parameters, making the controller parameter tuning range larger that it can control plant more flexible to obtain better control effects, however it also increases the difficulty of parameter selection. There has not been unified tuning method of parameters. In this paper, particle swarm optimization was used to optimize the parameters of seeking global optimal solution. Simulation results show that the performance of multivariable PI predictive functional controller was significantly better than predictive functional controller. [9]

The rest of this paper is organized as follows. Section Ⅱ derives Multivariable predictive functional control algorithm based on state-space equations. Section Ⅲ derives Multivariable PI predictive functional control algorithm based on state-space equations and proofs the robust stability of the improved algorithm. Section Ⅳ designs attitude controller of Near-space vehicle. Section Ⅴ simulation on the above two algorithms and compare it. Finally, section Ⅵ concludes this paper.

2. Multivariable Predictive Functional Control Algorithm Based On State-Space Equations

2.1. Base Functions and Predictive Model

For N input N output multivariable system, taking step function as base function, then the control input of the $(k+i)T$ can be written as

$$U(k+i)=\begin{bmatrix} u_1(k+i) \\ u_2(k+i) \\ \vdots \\ u_n(k+i) \end{bmatrix}=\begin{bmatrix} \mu_1 \\ \mu_2 \\ \vdots \\ \mu_n \end{bmatrix} \tag{1}$$

By the nature of step function that $U(k+i)=U(k)$

Where $i=1,2\text{L}$, $n=1\text{L}\ N$.

Take the state space equations as predictive model:

$$\begin{cases} X_m(k)=A_m X_m(k-1)+B_m U(k-1) \\ Y_m(k)=C_m X_m(k) \end{cases} \tag{2}$$

Where:

$$X_m(k)=[x_{m1}(k),x_{m2}(k)\cdots x_{mn}(k)]^T, U(k)=(u_1(k),u_2(k)\cdots u_n(k)),$$
$$Y_m(k)=[y_{m1}(k),y_{m2}(k)\cdots y_{mn}(k)]^T,$$

A_m , B_m , C_m are coefficient matrixes of state space equations.

According to the recursive principle predictive output at $(k+p)T$ can be derived by the formula (2)

$$Y_m(k+p)=C_m X_m(k+p)=C_m A_m^p X_m(k)+(C_m A_m^{p-1}B_m+C_m A_m^{p-2}B_m+\cdots+C_m B_m)U(k)=C_m A_m^p X_m(k)+G_p U(k)$$

where $G_p=(C_m A_m^{p-1}B_m+C_m A_m^{p-2}B_m+\cdots+C_m B_m)$, p is predictive steps.

As the effect of unmatched model and noise, existing certain error in model predictive output and process output.

$$\dot{e}(k+i)=\dot{e}(k)=Y_p(k)-Y_m(k) \tag{3}$$

Where: $\dot{e}(k+i)=[e_1(k+i),e_2(k+i),\cdots,e_n(k+i)]^T$, $\dot{e}(k)=[e_1(k),e_2(k),\cdots,e_n(k)]^T$,

$Y_p(k)=[y_{p1}(k),y_{p2}(k)\cdots y_{pn}(k)]^T$, $e_n(k+i)=e_n(k)=y_{pn}(k)-y_{mn}(k)$

Then the predictive model in $(k+p)T$ has been amended to $\hat{Y}_m(k+p)=Y_m(k+p)+\dot{e}(k+i)$

let $Y_p(k+p)=\hat{Y}_m(k+p)$

2.2. Optimization Calculation

In the PFC, in order to make the output of the system reaches the set value gently, regulating a curve called reference trajectory which progressive trend in set point. Take first-order exponential form as reference trajectory.

$$Y_r(k+i)=c(k+i)-(c(k)-Y_p(k))g\lambda^i=c(k)-(c(k)-Y_p(k))g\lambda^i \tag{4}$$

where $c(k)$ is set point, $c(k)=[c_1(k),\mathrm{L},c_n(k)]^T$, $\lambda^i=[\lambda_1^i,\mathrm{L},\lambda_n^i]$, $\lambda_n=e^{-T_s/T_{rn}}$

$y_{rn}(k+i)$ is the n[th] input reference trajectory in $(k+i)T$, $y_{pn}(k)$ is the n[th] input process output in kT, T_s is the sample time, T_{rn} is the expected response time of n[th] input reference trajectory.

The goal function of PFC takes the form of quadratic performance index:

$$J_p=\min\left\{\sum_{j=1}^{n}\left[y_{pj}(k+p)-y_{rj}(k+p)\right]^2\right\} \tag{5}$$

Let $J_p=0$, then obtained the expression of controlled variable

$$U(k)=G_p^{-1}\left[K_0C(k)-K_0Y_p(k)+K_1X_m(k)\right] \tag{6}$$

Where $K_0=\begin{bmatrix}1-\lambda_1^p & 0 & 0\\ 0 & \ddots & 0\\ 0 & 0 & 1-\lambda_n^p\end{bmatrix}$, $K_1=C_m-C_mA_m^p$

3. Multivariable PI Predictive Functional Control Algorithm Based On State-Space Equations

3.1. Derivation of Multivariable PI Predictive Functional Control Algorithm

Multivariable predictive functional control algorithm based on state-space equations deduced from Section II can be seen that it is relatively simple and less calculation on line. While it lack of flexibility because of there is only two adjustable parameters which is p and λ_n. Therefore improved the predictive functional control algorithm through combing the PFC quadratic performance index with PI, and then obtained new control algorithm—multivariable PI prediction functional control (MPIPFC) algorithm. The new control

algorithm has the structural features of proportional and integral in broadly that enhancing the flexibility of the algorithm. Take the objective function of MPIPFC as

$$J = \min_{U(k)}(K_i \cdot \hat{E}(k)^T \cdot Q \cdot \hat{E}(k) + K_p \cdot \Delta\hat{E}(k)^T \cdot Q \cdot \Delta\hat{E}(k) + U(k)^T RU(k)) \tag{7}$$

Where Q, R is error weighting factor and control variable weighting factor respectively, also they are positive definite matrixes. K_p, K_i is proportional and integral coefficient matrix respectively. $\hat{E}(k)$ is prediction error and $\Delta\hat{E}(k)$ is prediction error increment.

$$\hat{E}(k) = [E(k+1)^T, E(k+2)^T, \cdots, E(k+p)^T]^T$$

$$\Delta E(k+i) = [E(k+i) - E(k+i-1)]$$

$$\Delta\hat{E}(k) = [\Delta E(k+1)^T, \Delta E(k+2)^T, \cdots, \Delta E(k+p)^T]^T$$

The errors in $(k+i)T$ can be expressed as

$$\begin{aligned} &E(k+i) = Y_p(k+i) - Y_r(k+i) = Y_m(k+i) + \dot{e}(k+i) - Y_r(k+i) \\ &= Y_m(k+i) + Y_p(k) - Y_m(k) - Y_r(k+i) = C_m A_m^i X_m(k) + G_i U(k) + Y_p(k) \\ &- C_m X_m(k) - (c(k) - (c(k) - Y_p(k))g\lambda^i) = G_i U(k) + D_i(k) \end{aligned} \tag{8}$$

Let

$$E(k+i) = [E_1(k+i), E_2(k+i), \cdots, E_n(k+i)]^T,$$

$$D_i(k) = (C_m A_m^i - C_m) X_m(k) + Y_p(k) - (c(k) - (c(k) - Y_p(k))g\lambda^i)$$

$$\hat{E}(k) = [E(k+1)^T, E(k+2)^T, \cdots, E(k+p)^T]^T = \begin{bmatrix} D_1(k) + G_1 U(k) \\ D_2(k) + G_2 U(k) \\ \vdots \\ D_p(k) + G_p U(k) \end{bmatrix} = D(k) + GU(k) \tag{9}$$

Where

$$D(k) = \left[D_1(k)^T, D_2(k)^T, \cdots, D_p(k)^T\right]^T, G = \left[G_1^T, G_2^T, \cdots, G_p^T\right]^T$$

By recursive principle we know

$$\hat{E}(k+1) = D(k+1) + GU(k+1)$$

$$\begin{aligned} &\Delta\hat{E}(k+1) = \hat{E}(k+1) - \hat{E}(k) = D(k+1) + GU(k+1) - \\ &(D(k) + GU(k)) = D(k+1) - D(k) + G(U(k+1) - \\ &U(k)) = \Delta D(k+1) + G \cdot \Delta U(k+1) \end{aligned}$$

In a similar way

$$\Delta\hat{E}(k) = \Delta D(k) + G \cdot \Delta U(k) \tag{10}$$

Abbreviated as

$$\hat{E} = D + G \cdot U, \Delta\hat{E} = \Delta D + G \cdot \Delta U$$

Then rewritten MPIPFC objective function (7) as

$$J = \min_{U(k)}(K_p \hat{E}^T Q \hat{E} + K_d \Delta\hat{E}^T Q \Delta\hat{E} + \mathrm{U}^T \mathrm{RU}) \tag{11}$$

Let $\frac{\partial J}{\partial U}=0$, Then

$$K_p(G^TQD+G^TQGU)+K_d(G^TQ\Delta D+G^TQG\Delta U)+RU=0 \tag{12}$$

Introduction of backward operator then

$$\Delta U=(1-q^{-1})U\ ,\ \Delta D=(1-q^{-1})D$$

Obtained the expression of controlled variable of MPIPFC

$$U=-\left[(K_p+K_i)G^TQG-K_pG^TQGq^{-1}+R\right]^{-1}\cdot\left[(K_p+K_i)G^TQD-K_pG^TQq^{-1}D\right]$$

Step function as the base function then

$$G^TQGq^{-1}=G^TQG$$

The final expression of MPIPFC control variable is

$$U=-\left[K_iG^TQG+R\right]^{-1}\cdot\left[(K_p+K_i)G^TQD-K_pG^TQq^{-1}D\right] \tag{13}$$

3.2. Robust Stability Analysis of MPIPFC

As the set point does not affect the stability of closed-loop system, we therefore let the set value $c(k)=[c_1(k),\mathrm{L}\ ,c_n(k)]^T=[0]_{n\times 1}$, MPIPFC control variable expression (13) can be written as the form of equation (14)

$$U(k)=-KX_m(k) \tag{14}$$

Where

$$K=\left[K_iG^TQG+R\right]^{-1}\left[(K_p+K_i)G^TQ-K_pG^TQq^{-1}\right]D_0\ ,\ D_0=\left[D_{10}^T,D_{20}^T,\cdots,D_{p0}^T\right]^T\ ,\ D_{i0}=C_mA_m^i-\lambda^iC_m$$

$$\lambda^i=diag\left[\lambda_1^i,\lambda_2^i,\cdots,\lambda_n^i\right],i=1,2,\cdots,p$$

In the actual control process, considering the uncertainty caused by external interference and model mismatch, the controlled plant model can be expressed as the following state-space equations.

$$\begin{cases}X(k+1)=AX(k)+BU(k)+\Phi\\ Y(k)=CX(k)\end{cases} \tag{15}$$

Where $X\in R^{n\times 1}$ is state variable, $U\in R^{m\times 1}$ is the controlled variable, $Y\in R^{m\times 1}$ is the output, A, B and C are the coefficient matrixes of the state equation, Φ is the uncertain of the system.

Substituting (14) into (15) can obtain system closed-loop equation as follows

$$X(k+1)=AX(k)-BKX(k)+\Phi \tag{16}$$

Theorem 1. For the uncertain system, if the uncertain meet

$$\frac{\|\Phi\|}{\|X(k)\|}<\rho \tag{17}$$

Then the obtained MPIPFC control law can guarantee the system asymptotically stable. Where ρ is defined as the degree of robustness of the system and given by

$$\rho = -\sigma_{\max}(A-BK) + \sqrt{\sigma_{\max}^2(A-BK) + \frac{\lambda_{\min}(N)}{\lambda_{\max}(M)}} \tag{18}$$

Where $\sigma_{\max}(\bullet)$ is the maximum singularity of the matrix $(\bullet)$, $\lambda_{\max}(\bullet)$ and $\lambda_{\min}(\bullet)$ is the minimum and maximum eigenvalue of the matrix $(\bullet)$ respectively. M and N are the symmetric positive definite matrices and satisfy the following Riccati equation

$$(A-BK)^T M(A-BK) - M = -N \tag{19}$$

Proof:

Define the following definite quadratic function as a Lyapunov function for the closed loop system (16)

$$V[X(k)] = X(k)^T MX(k) \tag{20}$$

Derivative of $V[X_m(k)]$, replace $V[X_m(k)]$ as $\dot{V}[X_m(k)]$

$$\begin{aligned}
&\Delta V[X(k)] = V[X(k+1)] - V[X(k)] = X^T(k+1)MX(k+1) - X^T(k)MX(k) \\
&= [AX(k) - BKX(k) + \Phi]^T M[AX(k) - BKX(k) + \Phi] - X^T(k)MX(k) \\
&= X^T(k)\left[(A-BK)^T M(A-BK) - M\right]X(k) + X^T(k)(A-BK)^T M\Phi + \Phi^T M(A-BK)X(k) + \Phi^T M\Phi
\end{aligned} \tag{21}$$

Substituting (19) into (21) leads to

$$\begin{aligned}
&\Delta V(X(k)) = -X^T(k)NX(k) + X^T(k)(A-BK)^T M\Phi + \Phi^T M(A-BK)X(k) + \Phi^T M\Phi \\
&< -\lambda_{\min}(N)\|X(k)\|^2 + 2\sigma_{\max}(A-BK)\lambda_{\max}(M)\|\Phi\|\cdot\|X(k)\| + \lambda_{\max}(M)\|\Phi\|^2 \\
&= \|X(k)\|^2\left[-\lambda_{\min}(N) + 2\sigma_{\max}(A-BK)\lambda_{\max}(M)\frac{\|\Phi\|}{\|X(k)\|} + \lambda_{\max}(M)\left(\frac{\|\Phi\|}{\|X(k)\|}\right)^2\right]
\end{aligned} \tag{22}$$

Let

$$\rho_1 = \frac{\|\Phi\|}{\|X(k)\|} > 0 \tag{23}$$

Then (22) changes into

$$\Delta V(X(k)) < \|X(k)\|^2\left[\lambda_{\max}(M)\rho_1^2 + 2\sigma_{\max}(A-BK)\lambda_{\max}(M)\rho_1 - \lambda_{\min}(N)\right] \tag{24}$$

It is known from (17), (18) and (23) that

$$\rho_1 = \frac{\|\Phi\|}{\|X(k)\|} < -\sigma_{\max}(A-BK) + \sqrt{\sigma_{\max}^2(A-BK) + \frac{\lambda_{\min}(N)}{\lambda_{\max}(M)}} = \rho \tag{25}$$

Due to $\rho_1 > 0$,then (25) can be expressed by

$$-\sigma_{\max}(A-BK) - \sqrt{\sigma_{\max}^2(A-BK) + \frac{\lambda_{\min}(N)}{\lambda_{\max}(M)}} < 0 < \rho_1 < -\sigma_{\max}(A-BK) + \sqrt{\sigma_{\max}^2(A-BK) + \frac{\lambda_{\min}(N)}{\lambda_{\max}(M)}} \tag{26}$$

Inequality (27) is the solution of the following quadratic inequality

$$\lambda_{\max}(M)\rho_1^2 + 2\sigma_{\max}(A-BK)\lambda_{\max}(M)\rho_1 - \lambda_{\min}(N) < 0 \tag{27}$$

From (24) we know that

$$\Delta V(X(k)) < 0$$

From the above derivation can be seen that the Lyapunov function monotonically decreasing in MPIPFC control law. Then the closed loop system is asymptotically stable within a certain range of uncertainty.

4. Spacecraft Attitude Controller Design

Since the flight state variables of near space vehicle (NSV) is very different in time scales, the attitude controller is divided into 2 loops: a fast loop and a slow loop according to singular perturbation theory [10]. Where the angle of attack α, side slip angle β, roll angle μ are variables in the slow loop, and the corresponding attitude angular rate ω (p, q, r) are variables in fast loop. NSV attitude control system structure was shown in figure 1.

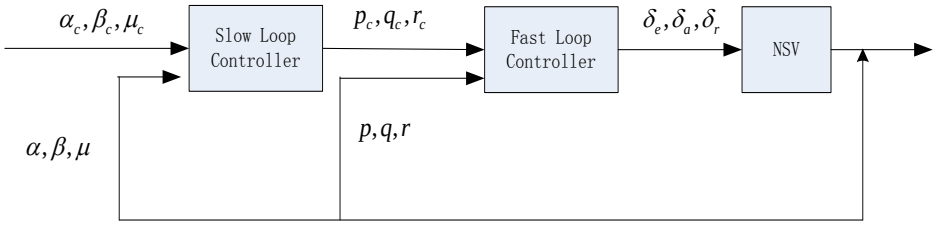

Figure 1: Attitude Control System Structure Of NSV

4.1. Slow Loop Controller Design

Slow loop consist of state variables α, β, μ .As the fast states transition process has ended and into steady-state process before the slow states began to respond, then we have $p = p_c$, $q = q_c$, $r = r_c$,the slow loop nonlinear equation:

$$\overset{g}{\Omega} = f_s + G_{s1}\omega \tag{28}$$

Where $f_s = [f_\alpha, f_\beta, f_\mu]^T$,specific expression :

$$f_\alpha = \frac{1}{MV\cos\beta}[-\hat{q}SC_{L,\alpha} + Mg\cos\gamma\cos\mu - T_x\sin\alpha]$$

$$f_\beta = \frac{1}{MV}[\hat{q}SC_{Y,\beta}\beta\cos\beta + Mg\cos\gamma\cos\mu - T_x\sin\beta\cos\alpha]$$

$$f_\mu = \frac{1}{MV}[\hat{q}SC_{Y,\beta}\beta\tan\gamma\cos\mu\sin\beta + L\tan\beta - Mg\cos\gamma\cos\mu\tan\beta + T_x[\sin\alpha(\tan\gamma\sin\mu + \tan\beta) - \cos\alpha\tan\gamma\cos\mu\sin\beta] + \hat{q}SC_{L,\alpha}(\tan\gamma\sin\mu + \tan\beta)$$

G_{s1} is a 3×3 matrix, the specific expression:

$$G_{s1} = \begin{bmatrix} -\tan\beta\cos\alpha & 1 & -\tan\beta\sin\alpha \\ \sin\alpha & 0 & -\cos\alpha \\ \sec\beta\cos\alpha & 0 & \sec\beta\sin\alpha \end{bmatrix}$$

Where M is NSV mass, V is air speed, S is the reference area of NSV wing surface, $\hat{q}$ is dynamic pressure, T_x is the compound force in x shift of engine thrust force, L is lift force, $C_{Y,\beta}$ and $C_{L,\alpha}$ is side and lift coefficient respectively, which is function of angle of attack and Mach.

The above equations show a strong nonlinearity, it will make the controller more complex and may lead to system instability if regard them as predictive model directly. To simplify the controller, linearized the nonlinear equations at an equilibrium point according the principle of small perturbations, and then take the linearization equations as predictive model. A balanced state of aircraft was selected

$$(\alpha_0 = 1^o, \beta_0 = 0^o, \mu_0 = 3^o, p_0 = 0^o, q_0 = 0^o, r_0 = 0^o)$$

Linearized the slow loop equations at the equilibrium and obtained a linear model near the equilibrium point:

$$\begin{cases} \overset{g}{x_1} = A_1 x_1 + B_1 u_1 \\ y_1 = C_1 x_1 \end{cases} \tag{29}$$

Where

$$x_1 = \Omega, \quad u_1 = \omega_c$$

$$A_1 = \begin{bmatrix} 0.0618 & -0.0002 & 0.0002 \\ 0.0002 & A-0.0382 & 0.0041 \\ 0 & 0.0578 & 0 \end{bmatrix} \quad B_1 = \begin{bmatrix} 0 & 1 & 0 \\ 0.0175 & 0 & -0.9998 \\ 0.9998 & 0 & 0.0175 \end{bmatrix}, \quad C_1 = \begin{bmatrix} 1 & 0 & 0 \\ 0 & 1 & 0 \\ 0 & 0 & 1 \end{bmatrix}$$

The slow loop MPIPFC control law can be obtained according to (13)

$$\omega_c = -\left[K_i G^T Q G + R\right]^{-1} \cdot \left[(K_p + K_i) G^T Q D - K_p G^T Q q^{-1} D\right] \tag{30}$$

4.2. The Fast Loop Controller Design

The fast loop nonlinear equations:

$$\overset{g}{\omega} = f_f + g_f M_c \tag{31}$$

Where $f_f = [f_p, f_q, f_r]^T$, the specific expression:

$$\begin{aligned} f_p &= [l_{aero} - qr(I_{zz} - I_{yy})] / I_{xx} \\ f_q &= [m_{aero} - pr(I_{xx} - I_{zz})] / I_{yy} \\ f_r &= [n_{aero} - pq(I_{yy} - I_{xx})] / I_{zz} \end{aligned}$$

g_f is a 3×3 matrix, the specific expression:

$$\mathrm{g}_f = \begin{bmatrix} I_{xx}^{-1} & 0 & 0 \\ 0 & I_{yy}^{-1} & 0 \\ 0 & 0 & I_{zz}^{-1} \end{bmatrix}$$

Where I_{xx}, I_{yy}, I_{zz} are moment of inertia, l_{aero}, m_{aero}, n_{aero} are decomposition of non-control torque in body coordinate system.

Similar to slow circuit design method, linearized the fast loop equations in the equilibrium point which is described in A of section Ⅳ:

$$\begin{cases} \overset{g}{x_2} = A_2 x_2 + B_2 u_2 \\ y_2 = C_2 x_2 \end{cases} \tag{32}$$

Where $x_2 = \omega, \quad u_2 = M_c$

$$A_2 = \begin{bmatrix} -0.0839 & 0 & 0.1029 \\ 0 & -2.0394 & 0.0002 \\ 0.0088 & -0.0002 & -0.0809 \end{bmatrix} \quad B_2 = \begin{bmatrix} 7.484e-007 & 0 & 0 \\ 0 & 7.5e-008 & 0 \\ 0 & 0 & 8.09e-008 \end{bmatrix}$$

$$C_2 = \begin{bmatrix} 1 & 0 & 0 \\ 0 & 1 & 0 \\ 0 & 0 & 1 \end{bmatrix}$$

The fast loop MPIPFC control law can be obtained according to (13)

$$M_c = -\left[K_i G^T Q G + R\right]^{-1} \cdot \left[(K_p + K_i) G^T Q D - K_p G^T Q q^{-1} D\right] \tag{33}$$

4.3. Control Allocation

Control torque obtained by fast loop can not directly on the aircraft, it would be allocated to every rudder surface though assignment matrix and then control the NSV. According to the literature [11] shows

$$M_c = g_{f,\delta}\delta \tag{34}$$

Where δ is rudder angle vector

$$\delta = \left[\delta_e, \delta_a, \delta_r, \delta_x, \delta_y, \delta_z\right]^T$$

$g_{f,\delta}$ is a 3×6 matrix

$$g_{f,\delta} = \begin{bmatrix} g_{p,\delta_e} & g_{p,\delta_a} & g_{p,\delta_r} & g_{p,\delta_x} & 0 & 0 \\ g_{q,\delta_e} & g_{q,\delta_a} & g_{q,\delta_r} & 0 & 0 & g_{q,\delta_z} \\ g_{r,\delta_e} & g_{r,\delta_a} & g_{r,\delta_r} & 0 & g_{r,\delta_y} & 0 \end{bmatrix}$$

The non-zero elements in $g_{f,\delta}$

$$g_{p,\delta_e} = \hat{q} S b C_{l,\delta_e}, g_{p,\delta_a} = \hat{q} S b C_{l,\delta_a}$$

$$g_{p,\delta_r} = \hat{q} S b C_{l,\delta_r}, g_{p,\delta_x} = -\frac{\pi}{180} T_x X_{rc}$$

$$g_{q,\delta_e} = \hat{q} S c C_{m,\delta_e} + X_{cg} \hat{q} S (C_{D,\delta_e} \sin\alpha + C_{L,\delta_e} \cos\alpha)$$

$$g_{q,\delta_a} = \hat{q} S c C_{m,\delta_a} + X_{cg} \hat{q} S (C_{D,\delta_a} \sin\alpha + C_{L,\delta_r} \cos\alpha)$$

$$g_{q,\delta_r} = \hat{q} S c C_{m,\delta_r} + X_{cg} \hat{q} S C_{D,\delta_r} \sin\alpha$$

$$g_{q,\delta_z} = \frac{\sqrt{2}\pi}{360} T (X_T - X_m), g_{r,\delta_e} = \hat{q} S b C_{n,\delta_e} + X_{cg} \hat{q} S C_{Y,\delta_e}$$

$$g_{r,\delta_a} = \hat{q} S b C_{n,\delta_a} + X_{cg} \hat{q} S C_{Y,\delta_a}, g_{r,\delta_r} = \hat{q} S b C_{n,\delta_r} + X_{cg} \hat{q} S C_{Y,\delta_r}$$

$$g_{r,\delta_y} = -\frac{\sqrt{2}\pi}{360} T (X_T - X_m)$$

Where X_T is the distance from main engine thrust center to edge, X_m is the distance from center of mass to the front edge, T is total thrust of engine, b is wingspan length, c is the mean aerodynamic chord length, X_{cg} is the distance from center to reference torque center, $C_{l,\delta_e}, C_{l,\delta_a}, C_{l,\delta_r}; C_{m,\delta_e}, C_{m,\delta_a}, C_{m,\delta_r}; C_{n,\delta_a}, C_{n,\delta_e}, C_{n,\delta_r}$ are the roll, pitch, yaw moment increment coefficient respectively that caused by the left and elevator aileron and rudder, $C_{Y,\delta_e}, C_{Y,\delta_a}, C_{Y,\delta_r}; C_{D,\delta_e}, C_{D,\delta_a}, C_{D,\delta_r}$ are lateral force and resistance increment

coefficient respectively that caused by the left and right movements aileron and rudder, C_{L,δ_e}, C_{L,δ_r} are the lift increment coefficient caused by the left and right elevator aileron. These aerodynamic coefficients are function of angle of attack and Mach.

4.4. Particle Swarm Optimization Tuning Parameters of the Fast and Slow Controllers

Multivariable PI predictive functional controller contains two factors K_p, K_i and two weighting coefficients Q, R. There are eight parameters need tuning in the controller which is designed in this paper. They are K_{p1}, K_{I1}, Q_1, R_1, K_{p2}, K_{I2}, Q_2, R_2 respectively. These eight parameters is proportional gain, integral gain, weighting coefficient of fast and slow loop respectively. Evaluated these eight parameters can be transformed into solving the optimal value problem. In this paper, optimized the eight parameters through particle swarm optimization (PSO) online and then assigned to the eight parameters with the found optimal control parameters.

The objective function of PSO takes the weighted sum of slow loop integrated time and absolute error (ITAE), as the following formula

$$J = w_1\int_0^\infty t\,|e_1|dt + w_2\int_0^\infty t\,|e_2|dt + w_3\int_0^\infty t\,|e_3|dt \tag{35}$$

Where $e_1 = \alpha - \alpha_c$, $e_2 = \beta - \beta_c$, $e_3 = \mu - \mu_c$

w_1, w_2, w_2 are weighting coefficients.

The relative size of w_1, w_2, w_2 reflect the degree of importance of the three outputs. In this paper, in order to ensure the three outputs identical importance, select the same weighting coefficient. To highlight the importance of one of the outputs, the output should be re-select the weighting coefficient to ensure the output can be tuned better and faster.

The settings of PSO optimized MPIPFC parameter: number of particles $m = 30$, dimension $\dim = 8$, learning factor $c_1 = c_2 = 2$, inertia weight $\omega = 0.9 - 0.5t/G_k$, the maximum number of iterations $G_k = 50$,fitness value $w_1 = 0.5$, $w_2 = 0.5$, $w_3 = 0.5$.

Optimization steps:

Step1. Initialize population, including the number of particles, number of iterations, learning factor, inertial factors, position and velocity of particles.

Step2. Calculate the fitness of each particle to determine the individual optimal location $P_i(t)$ and group best position $P_g(t)$.

Step3. Update the position and velocity of each particle.

Step4. Update the individual and group optimal values.

Step5. Iteration t plus one, update ω.

Step6. If t is larger than the maximum number of iterations, then execute Step7, or returned to Step3.

Step7. The final group optimal values are the obtained optimal parameters.

5. Aircraft Simulation

Aircraft model and aerodynamic parameters are from report of NASA [12]. When simulation, taking the flight speed of NSV Mach eight, height $H = 27km$,the thrust of engine was kept $T = 28kN$. The initial attitude angle of NSV is

$\alpha = 0^o$, $\beta = 0^o$, $\mu = 1^o$, $p = 0^o$, $q = 0^o$, $r = 0^o$, attitude command signal $\alpha_c = 1^o$, $\beta_c = 0^o$, $\mu_c = 3^o$. Requires each rudder angle limiter are

$0^\circ < \delta_e, \delta_a, \delta_r < 30^\circ, 0^\circ < \delta_x, \delta_y, \delta_z < 15^\circ$. Simulations of predictive functional control algorithm and multivariable PI predictive functional control algorithm are carried out. The response curves of NSV attitude control system are shown in Figure 2-4, which double dash line represents the expected curve, the solid line represents the simulation curve of MPIPFC controller, dotted line represents the simulation curve of PFC controller.

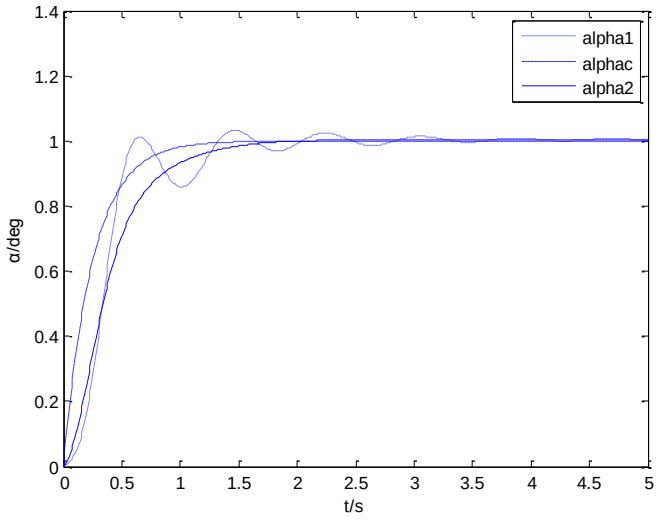

Figure 2: Track Curves of Attack Angle

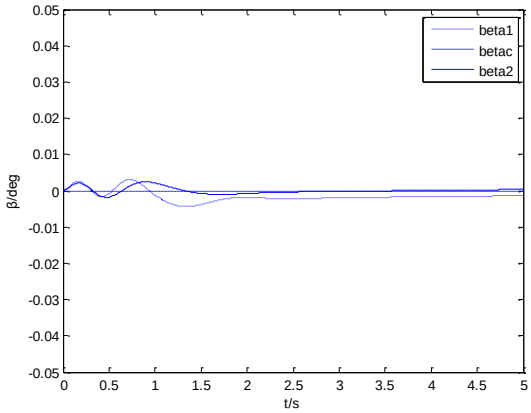

Figure 3: Track Curves of Sideslip Angle

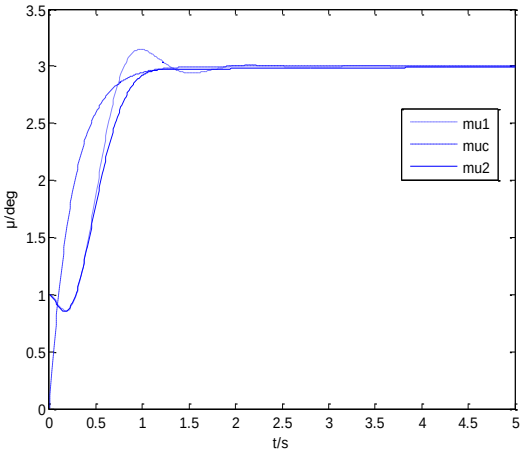

Figure 4: Track Curves of Roll Angle

The following six figures show the response curve of the NSV attitude control rudder angle.

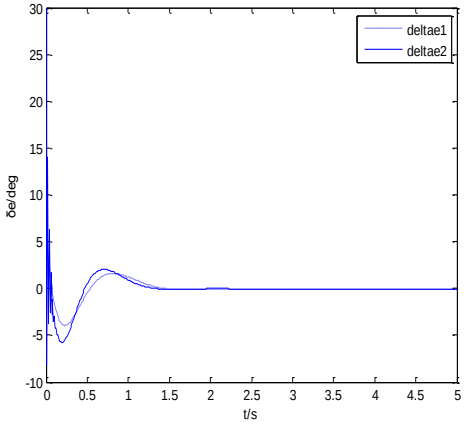

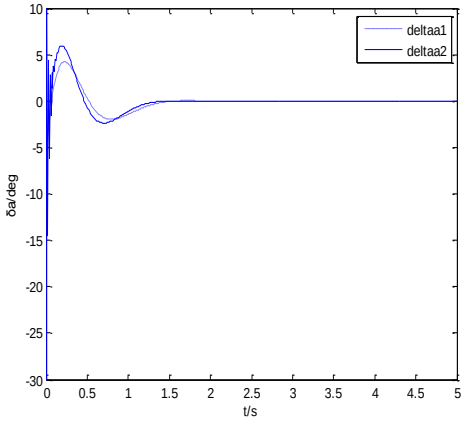

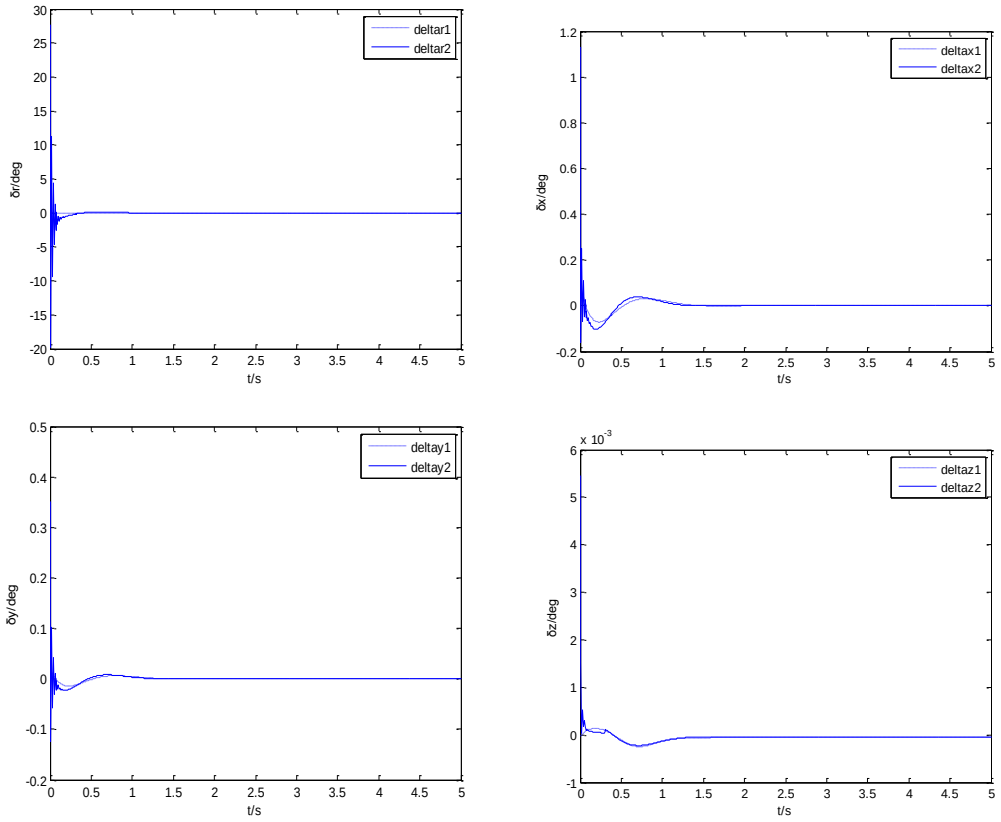

As can be seen from the figure 2-4, the two control algorithms are capable of achieving good control, while the PFC simulation curves have overshoot and shock more frequently. MPIPFC overcome the shortcomings of the PFC. From the control surface deflection angle response curve can be seen rudder angle without saturating.

6. Conclusions

In this paper, a NSV attitude controller is designed. The plant with non-linear and strong coupling was controlled by predictive functional control algorithm and multivariable PI predictive functional control algorithm. Tuning the parameter by genetic optimization algorithm. Simulation results show that the two algorithms can both achieve satisfactory control effects. The performance of multivariable PI predictive functional control is better by contrast, for it has the advantage of no overshoot and less static state error etc.

Acknowledgments

This paper is a revised and expanded version of a paper entitled "Research on the multivariable predictive functional control algorithm based on the state space equation" presented at CST 2015, Suzhou, China, April 23-25, 2015. This work was supported by National Natural Science Foundation of China (61104062, 61374085, 61473334, 614022342), Jiangsu Qing Lan Project, the Industrial Strategic Technology Development Program (10041740) funded by the Ministry of Trade, Industry and Energy (MOTIE) Korea and PAPD.

7. References

7.1. Journal Article

[1] Fidan B, Mirmirani M and Ioannou P A. "Flight dynamics and control of air-breathing hypersonic vehicles: review and new directions".*12th AIAA International Space Planes and Hypersonic Systems and Technologies, Norfolk, USA, AIAA 2003-7081*, pp.1-24.
[2] Cui Erjie. "Research statutes, development trends and key technical problems of near space flying vehicles" *Advances in Mechanics*, vol.39, no.6, pp.658-673, 2009.
[3] Zkan L and Kothare M V." Stability analysis of a multi-model predictive control algorithm with application to control of chemical reactors ". *Journal of Process Control* , vol.16, no.2, pp.81-90,**2006**
[4] Curt is Zimmerman. An automated method to compute orbital re-entry trajectories with heating constraints[. Guidance, Navigation, and Control Conference and Exhibit ,AIAA 2002- 4454
[5] Hyochoong B. "Predictive control for the attitude maneuver of a flexible spacecraft". *Aerospace Science and Technology*, vol.8, no. 1, pp. 443- 452, **2004**.
[6] Fang Wei and Jiang Changsheng. "Design of a Predictive Control Law for Re-entry Aerospace Vehicles ".*Systems Engineering and Electronics*, vol. 29 no.8, pp.1317-1321,**2007**
[7] Huixian Liu and Shihua Li. "Speed control for PMSM servo system using predictive functional control and extended state observer". *IEEE Transactions on Industrial Electronics*, vol.59, no.2, pp.1171-1183, **2012**.
[8] Naidu N S, and Calise A J. "Singular Perturbations and Time Scales in Guidance and Control of Aerospace Systems: A Survey", *Journal of Guidance, Control and Dynamics*, vol.24, no. 6, pp.1057-1078, **2001**.
[9] Jin Wang, Jeong-Uk Kim, Lei Shu, Yu Niu and Sungyoung Lee, A distance-based energy aware routing algorithm for wireless sensor networks, Sensors, Vol.10, No.10, **2010**, pp.9493-9511.
[10] Jin Wang, Yue Yin, Jianwei Zhang, Sungyoung Lee, and R. Simon Sherratt, Mobility based energy efficient and multi-sink algorithms for consumer home networks, IEEE Transactions on Consumer Electronics, Vol.59, No.1, Feb. **2013**, pp.77-84.
[11] Richang Hong, Jianxin Pan, Shijie Hao, Meng Wang, Feng Xue and Xindong Wu: Image quality assessment based on matching pursuit. Inf. Sci., **2014**, pp.196-211.
[12] Richang Hong, Wenyi Cao, Jianxin Pang and Jianguo Jiang: Directional projection based image fusion quality metric. Inf. Sci., **2014**, pp.611-619.

5.2. Conference Proceedings and Dissertation

[13] Yiming Song and Bin Yang. "Cascade temperature control for bench-scale batch reactor an application of predictive functional control technique". *Proceeding of the 10th World Congress on Intelligent control and Automation.* **2012**, pp.1564-1569.
[14] Zhao Jiang. Study on Multivariable Predictive Functional Control and Its Applications. Zhejiang. Department of Control Science and Engineering Institute of Advanced Process Control. **2006**:27-33.
[15] Zhu Liang. "Robust adaptive control for uncertain nonlinear systems and its applications to aerospace vehicles". *Nanjing University of Aeronautics and Astronautics the Graduate School College of Automation Engineering.* **2006**, pp.24-26.
[16] Shariar K. "Six-DOF modeling and simulation of a generic hypersonic vehicle for conceptual design studies". *Modeling and Simulation Technologies Conference. AIAA*:2004-4805.

Authors

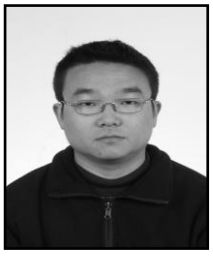

Zhenyu Lu received Ph. D. degree in optical engineering at Nanjing University of Science and Technology, Nanjing, China in 2008. His research interests include intelligent control and the stochastic control.

Kai Li receive the B.S in the Changzhou University, China in 2012. He is pursuing MS. degree in Nanjing University of Information Science and Technology, Nanjing, China. His research interests include optimal control.

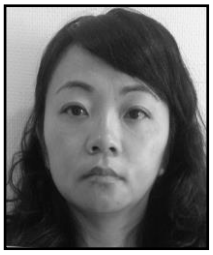

Tingya Yang received MS. degree at Nanjing University of Information Science and Technology, Nanjing, China in 2005. Her research interests include signal processing.

Wei Guo received his MS degree in 1987 from Shandong University. His main research interests include intelligent control and Smart grid.